Molecular Biology of the Cell
Vol. 9, 1919–1938, July 1998

Isolation and Contraction of the Stress Fiber

Kazuo Katoh,* Yumiko Kano, Michitaka Masuda, Hirofumi Onishi, and Keigi Fujiwara

Department of Structural Analysis, National Cardiovascular Center Research Institute, Suita, Osaka 565-8565, Japan

Submitted October 3, 1997; Accepted April 29, 1998
Monitoring Editor: Paul Matsudaira

Stress fibers were isolated from cultured human foreskin fibroblasts and bovine endothelial cells, and their contraction was demonstrated in vitro. Cells in culture dishes were first treated with a low-ionic-strength extraction solution and then further extracted using detergents. With gentle washes by pipetting, the nucleus and the apical part of cells were removed. The material on the culture dish was scraped, and the freed material was forced through a hypodermic needle and fractionated by sucrose gradient centrifugation. Isolated, free-floating stress fibers stained brightly with fluorescently labeled phalloidin. When stained with anti-α-actinin or anti-myosin, isolated stress fibers showed banded staining patterns. By electron microscopy, they consisted of bundles of microfilaments, and electron-dense areas were associated with them in a semiperiodic manner. By negative staining, isolated stress fibers often exhibited gentle twisting of microfilament bundles. Focal adhesion–associated proteins were also detected in the isolated stress fiber by both immunocytochemical and biochemical means. In the presence of Mg-ATP, isolated stress fibers shortened, on the average, to 23% of the initial length. The maximum velocity of shortening was several micrometers per second. Polystyrene beads on shortening isolated stress fibers rotated, indicating spiral contraction of stress fibers. Myosin regulatory light chain phosphorylation was detected in contracting stress fibers, and a myosin light chain kinase inhibitor, KT5926, inhibited isolated stress fiber contraction. Our study demonstrates that stress fibers can be isolated with no apparent loss of morphological features and that they are truly contractile organelle.

INTRODUCTION

Stress fibers are needle-shaped bundles of actin filaments. By immunolabeling, they are shown to also contain various actin-associated proteins such as myosin, tropomyosin, and α-actinin, to name a few (Byers *et al.*, 1984; Burridge *et al.*, 1988). Together with actin filaments, these proteins are thought to be organized into a sarcomere-like structure (Sanger, 1980; Langanger *et al.*, 1986). The stress fiber is also thought to generate tension. Contraction of detergent-extracted cell models consisting of stress fibers and actin filaments in the cell cortex occurred when Mg^{2+} and ATP were added (Hoffmann-Berling, 1954; Kreis and Birchmeier, 1980). Microlaser-dissected stress fibers still associated with the plasma membrane, and the cortex of cultured cells contracted upon the addition of Mg^{2+} and ATP (Isenberg *et al.*, 1976). Although these demonstrations suggest contraction of stress fibers, these in vitro systems contain the cell cortex, which may also be contractile. Cells grown in or on flexible matrices can deform the matrix, and stress fiber contraction was thought to be responsible for this (Harris *et al.*, 1981; Mochitate *et al.*, 1991). However, similar matrix contraction could be induced without stress fibers (Mochitate *et al.*, 1991; Halliday and Tomasek, 1995). These latter studies indicate that the cell cortex itself is highly contractile. Thus, although there is circumstantial evidence suggesting contractile force production by stress fibers, it should be noted that there exists no direct evidence that stress fibers themselves are contractile.

To demonstrate stress fiber contractility without any ambiguity, it is necessary to show contraction of stress

* Corresponding author.

fibers that are free of other possibly contractile components of the cell. Thus, isolation of stress fibers from cultured cells was planned. Because stress fibers are abundant in the basal portion of cultured cells, our strategy for isolating stress fibers was to first remove the apical cell portion. Several investigators have attempted to isolate structures associated with the basal plasma membrane, such as focal adhesions, and have met with limited success. In most of these methods, a stream of buffer was used to remove the dorsal region of cells and the soluble materials in the cytoplasm (Badley *et al.*, 1978; Cathcart and Culp, 1979; Avnur and Geiger, 1981; Avnur *et al.*, 1983; Neyfakh and Svitkina, 1983; Ball *et al.*, 1986; Nicol and Nermut, 1987). Others tried "wet-cleaving" using nitrocellulose membranes (Brands and Feltkamp, 1988). Some efforts have been made to do mass isolation of stress fibers, but isolated stress fibers were heavily contaminated with the cell cortex (Fujiwara *et al.*, 1985). The fact that isolation of stress fibers, unlike that of the brush border (Mooseker and Tilney, 1975), the circumferential marginal band (Owaribe and Masuda, 1982), and the contractile ring (Yonemura *et al.*, 1991), has been difficult appears to be their tight association with the cell cortex (Fujiwara *et al.*, 1985).

In this paper, we report a mass isolation procedure of stress fibers from cultured cells and show that they are contractile. This isolation method is a combination of low-ionic-strength extraction and selective detergent extraction. Isolated stress fibers were free of the cell cortex, although they were still associated with some extracellular matrix materials. When isolated stress fibers were exposed to Mg-ATP, rapid contraction was observed. Microbeads on contracting stress fibers rotated, indicating that rotational force was generated during stress fiber contraction. This contraction depended on the phosphorylation state of the myosin regulatory light chain, and indeed both calmodulin and myosin light chain kinase were associated with isolated stress fibers.

MATERIALS AND METHODS

Cell Culture

Human foreskin fibroblasts (FS-133) and bovine carotid arterial endothelial cells were cultured by using a 1:1 mixture of DMEM and nutrient mixture F-12 (Life Technologies, Grand Island, NY) (pH 7.4) containing 50 U/ml penicillin, 50 μg/ml streptomycin, and 10% fetal bovine serum (Salmond Smith Biolab, Auckland, New Zealand) (Sunada *et al.*, 1993). The cells were maintained at 37°C in a humidified 5% CO_2 atmosphere.

Isolation of Stress Fibers

FS-133 and endothelial cells were cultured for 3–4 d in culture dishes (150 × 150 mm; Greiner, Frickenhausen, Germany). Cells were briefly washed in an ice-chilled PBS and then treated with a low-ionic-strength extraction solution consisting of 2.5 mM triethanolamine (TEA; Wako, Osaka, Japan), 20 μg/ml Trasylol (Bayer, Leverkusen, Germany), 1 μg/ml leupeptin (Peptide Institute, Osaka, Japan), 1 μg/ml pepstatin (Peptide Institute), and 20 μg/ml [*N*-(L-3-*trans*-carboxyoxiran-2-carbonyl)-L-leucyl]amino (4-guanido) butane (E-64; Peptide Institute) (pH 8.2) at 4°C. With gentle agitation, cells were treated with the low-ionic-strength extraction solution for 10–40 min until the dorsal side of the cell became free floating. Extracted cells were then treated with extraction buffer I (0.05% NP-40 [BDH, Poole, United Kingdom], 20 μg/ml Trasylol, 1 μg/ml leupeptin, 1 μg/ml pepstatin, and 20 μg/ml E-64 in PBS, pH 7.2) for 5 min. Some cells at this stage still had the dorsal side and/or the nucleus, which were then removed by gentle shearing under a phase-contrast microscope with a stream of extraction buffer I. The material still attached to culture dishes was gently washed by extraction buffer II (0.05~0.5% Triton X-100 [Wako], 20 μg/ml Trasylol, 1 μg/ml leupeptin, 1 μg/ml pepstatin, and 20 μg/ml E-64 in PBS, pH 7.2). The extracted material was scraped off from the dish, suspended in extraction buffer II, and forced through an injection needle twice (23 gauge; Termo, Tokyo, Japan). This last procedure freed stress fibers from the sheet-like structure, presumably the cell cortex.

The crude stress fiber isolates were suspended in PBS containing 20 μg/ml Trasylol, 1 μg/ml leupeptin, 1 μg/ml pepstatin, and 20 μg/ml E-64 (pH 7.4) and centrifuged at 100,000 × *g* for 1 h. The pellet contained highly concentrated stress fibers sufficient for morphological studies. For further purification of stress fibers, sucrose gradient centrifugation was performed. A step gradient of 1.5, 1.2, and 1.0 M sucrose in 500 mM NaCl, 3 mM $MgCl_2$, 10 mM piperazine-*N*,*N*′-bis(2-ethanesulfonic acid) (Wako), and 1 mM EGTA (Wako) (pH. 7.4) was made, and samples were centrifuged for 60 min at 100,000 × *g*. Isolated and purified stress fibers were recovered in the 1.2 M sucrose fraction as well as at the 1.2–1.5 M interface.

Electron Microscopy

For thin-section electron microscopy, isolated stress fibers were collected by centrifugation and fixed with 2.5% glutaraldehyde and 2% paraformaldehyde in 0.1 M sodium cacodylate buffer (pH 7.4) for 30 min at room temperature. Fixed stress fibers were washed for 30 min in 0.1 M sodium cacodylate buffer and post-fixed for 1 h with 1% OsO_4 in the same buffer at 4°C. Samples were dehydrated through a graded series of ethanol (50, 65, 75, 85, 95, 99, and 100%) and embedded in Epon 812. Thin sections were stained with uranyl acetate and lead citrate.

For negative staining of isolated stress fibers, a drop of solution containing isolated stress fibers was put on a grid covered with Formvar film. After 2 min, the grid was rinsed and negatively stained with 4% uranyl acetate. After removal of the excess solution with a filter paper, the grid was quickly dried and examined.

For replica electron microscopy, stress fibers on glass coverslips were fixed with 1% glutaraldehyde, dehydrated through graded concentrations of ethanol (50, 65, 75, 85, 95, and 99%) and 2-methyl-2-propanol (99%), and then freeze dried. Samples were rotary shadowed with platinum/carbon at an angle of 45° in a JFD-9000 freeze fracture apparatus (JEOL, Tokyo, Japan). Replicas were detached from glass by brief treatment with 10% hydrofluoric acid and mounted on Formvar film-covered grids. Samples were examined using a JEOL 2000FX electron microscope at an accelerating voltage of 80 kV.

Antibodies

Polyclonal antibodies against α-actinin were made against chicken gizzard α-actinin (Fujiwara *et al.*, 1978). The following monoclonal antibodies were purchased: anti-α-smooth muscle actin (Sigma Chemical, St. Louis, MO), anti-pan-myosin (Amersham, Buckinghamshire, United Kingdom), anti-myosin light chain kinase (Sigma), anti-myosin regulatory light chain (Sigma), anti-calmodulin (Upstate Biotechnology, Lake Placid, NY), anti-vinculin (Sigma),

anti-talin (Sigma), anti-paxillin (Zymed, San Francisco, CA), anti-vimentin (Sigma), anti-pp125^{FAK} (Transduction Laboratories, Lexington, KY), anti-α-fodrin (ICN, Costa Mesa, CA), and anti-α-spectrin (our own). Polyclonal anti-fibronectin receptor (integrin $\alpha_5\beta_1$; Chemicon) was also purchased.

Immunofluorescence Microscopy

Cells on glass coverslips were washed in PBS and fixed with 1% paraformaldehyde in PBS for 15 min at room temperature. TEA-treated and detergent-extracted cells on coverslips were also fixed with 1% paraformaldehyde in PBS for 15 min and stained with several specific antibodies (see below). For staining isolated stress fibers, they were fixed with 1% paraformaldehyde in PBS for 15 min at room temperature, placed on poly-D-lysine (Sigma)–coated slide glasses for 2 min at 4°C, and washed in PBS. To quench unoccupied and nonspecific protein binding sites, slide glasses were treated with 10% normal goat serum for 1 h at room temperature. The above samples were stained with anti-myosin (dilution, 1:100), anti-α-actinin (1:200), anti-myosin light chain-kinase (1:100), anti-calmodulin (1:100), anti-vinculin (1:400), anti-talin (1:100), anti-paxillin (1:100), anti-vimentin (1:200), anti-pp125^{FAK} (1:100), or anti-fibronectin receptor (1:100) for 90 min. After being washed in PBS, samples were incubated with fluorescein (Cappel, Durham, NC)-, rhodamine (Cappel)-, or Texas Red (EY Lab, San Mateo, CA)-labeled goat anti-rabbit or anti-mouse immunoglobuliln (IgG). Some specimens were double stained with one of the antibodies (and the appropriate secondary antibody) and with rhodamine (Molecular Probe, Eugene, OR)- or fluorescein (Sigma)-labeled phalloidin.

Specimens were observed using a Zeiss Axiophot (Carl Zeiss, Oberkochen, Germany) epifluorescence microscope with an apochromat 63× (numerical aperture [NA] 1.4, oil) or a plan-neofluar 40× (NA 0.75) objective lens. Fluorescent images were photographed by using Kodak T-Max 400 film (Eastman Kodak, Rochester, NY).

SDS-PAGE and Immunoblotting

Isolated stress fibers were boiled for 3 min in the SDS-PAGE sample buffer (Laemmli, 1970) and electrophoresed on 10% polyacrylamide gels according to the method of Laemmli (1970). Gels were stained with Coomassie brilliant blue R-250 or using a silver staining kit (Wako). For quantitating SDS-gel band staining intensity, gels were stained with SYPRO-orange (Molecular Probes), and relative amounts of proteins were quantitated by an FLA-2000 fluorescent image analyzer (Fujifilm, Tokyo, Japan). For immunoblotting, polypeptide bands in an SDS-PAGE gel were electrophoretically transferred to a piece of nitrocellulose paper (Millipore, Bedford, MA; 0.45-μm pore size). The paper was treated with 10% nonfat dry milk in Tris-buffered saline (TBS; pH 7.4) and then incubated with rabbit anti-α-actinin (dilution, 1:1000), monoclonal anti-α-smooth muscle actin (1:200), anti-myosin (1:200), anti-myosin light chain kinase (1:500), anti-myosin regulatory light chain (1:500), anti-calmodulin (1:500), anti-vinculin (1:1000), anti-talin (1:100), anti-fibronectin receptor (1:500~1000), anti-pp125^{FAK} (1:200), anti-α-fodrin (1:500), or anti-α-spectrin (hybrydoma supernatant). Filter papers were washed in TBS, and bound antibodies were visualized by using a horseradish peroxidase-conjugated avidin–biotin complex system (Vector, Burlingame, CA) and a Konica (Tokyo, Japan) immunostain kit or an ECL kit (Amersham).

Contraction of Isolated Stress Fibers

To study contraction of isolated stress fibers, we made two types of isolated stress fiber preparations: TEA-treated and detergent-extracted stress fibers that were still attached to a coverslip (attached stress fibers) and free stress fibers that were obtained after sucrose gradient centrifugation (fractionated stress fibers). To induce contraction, they were first immersed in a wash solution (10 mM imidazole, 100 mM KCl, and 2 mM EGTA) (Owaribe and Masuda, 1982). Fractionated stress fibers were mounted on slide glasses. The attached and the fractionated stress fibers were perfused with a Mg-ATP solution (0.1 mM ATP, 3 mM $MgCl_2$, 1 mM $CaCl_2$, 1 mM EGTA, 75 mM KCl, and 20 mM imidazole, pH 7.2) (Owaribe and Masuda, 1982) and observed under a phase-contrast microscope (Zeiss Axiophot with a plan-neofluar 63×, NA 1.25, oil, Ph 3, antiflex objective lens) equipped with a video-enhanced imaging system.

The video system consisted of a high-resolution charge-coupled device TV camera (C2400–77; Hamamatsu Photonics, Hamamatsu, Japan) connected to a digital image processor (Image Sigma-II; Nippon Avionics, Tokyo, Japan), and images were recorded by a high-resolution laser video disk recorder (LV-250H; TEAC, Tokyo, Japan). To examine ATP dose dependence of stress fiber shortening, a range of ATP concentrations (0.005–0.1 mM) was used. Nucleotide specificity for contraction was examined by replacing 0.1 mM ATP in the Mg-ATP solution with GTP, UTP, CTP, ADP, GDP, or adenosine 5′-(β,γ-imino)triphosphate (AMP-PNP). To examine Ca^{2+} dependency of the isolated stress fiber contraction, stress fibers were incubated with a Ca^{2+}-free Mg-ATP solution containing 0.1 mM ATP, 10 mM imidazole, 100 mM KCl, 2 mM EGTA, and 3 mM $MgCl_2$ (pH 7.2). Relaxation of fractionated stress fibers was examined by washing contracted stress fibers with the Mg-ATP solution containing 2 mM EGTA and no $CaCl_2$.

To analyze the mode of contraction, attached stress fibers were first incubated with polystyrene microparticles (18190; Polysciences, Warrington, PA) for 5 min and rinsed by a wash solution. Conditions were determined so that, on average, one to five beads were attached to one stress fiber. Movement of microbeads during isolated stress fiber shortening was recorded by the video-enhanced phase-contrast system described above.

Phosphorylation of the Myosin Regulatory Light Chain

To study the effect of the myosin regulatory light chain phosphorylation on stress fiber contraction, stress fibers were pretreated with 0, 50, 100, 1000, or 5000 nM KT5926 (Nakanishi *et al.*, 1990) (Calbiochem, La Jolla, CA) in 75 mM KCl, 3 mM $MgCl_2$, 1 mM $CaCl_2$, 1 mM EGTA, and 20 mM imidazole (pH 7.2) for ≥30 min on ice before Mg-ATP (0.01 mM [γ-^{32}P]ATP [7.4 GBq/mM; Amersham], 3 mM $MgCl_2$, 1 mM $CaCl_2$, 1 mM EGTA, 75 mM KCl, and 20 mM imidazole, pH 7.2) addition. Phosphorylation of the myosin regulatory light chain was determined autoradiographically by using a Fujifilm BAS-5000 image analyzer.

RESULTS

Isolation and Morphology of Stress Fibers

Cells were first treated with a low-ionic-strength solution containing TEA. During this procedure, membrane-bound organelles and soluble materials of the cytoplasm were gradually extracted. Gentle shearing of cells with a stream of extraction buffer I selectively removed the nucleus and the dorsal side of the cell that was made fragile by TEA treatment. Stress fibers and some sheet-like structures remained on the substrate surface after the treatment with extraction buffer I. Washing this material with extraction buffer II removed practically all of the sheet-like structures and the remaining cytoplasm. The material attached to the substrate surface was removed by using a rubber policeman and forced through a 23-gauge needle. This last step was necessary for obtaining free-floating in-

dividual stress fibers. This crude stress fiber preparation was fractionated by sucrose gradient centrifugation. Because the length and the thickness of stress fibers were quite variable, isolated stress fibers were enriched in the 1.2 M sucrose layer as well as at the 1.2–1.5 M interface as mentioned in MATERIALS AND METHODS. A small number of nuclei and large cell fragments formed a pellet at the bottom of centrifuge tubes.

Figure 1 shows electron micrographs of negatively stained isolated stress fibers from bovine endothelial cells (Figure 1, a–c) or FS-133 (Figure 1d). An isolated stress fiber was a bundle of microfilaments and, no membranes and organelles were associated with it. At higher magnifications, ~5-nm individual filaments were seen as strings of globular actin molecules (Figure 1, c and d). Depending presumably on the direction from which a stress fiber is observed, widening of ends was observed (Figure 1a). At the end of a stress fiber, the actin filament bundle split into several finger-like projections (Figure 1d). We often found that the microfilament bundle of isolated stress fibers gently twisted (Figure 1, a and b).

Transmission electron micrographs of the isolated stress fiber fraction showed bundles of microfilaments with some electron-dense structures associated with them (Figure 2). When a single bundle of microfilaments was transversally sectioned, electron-dense regions were observed in a semiperiodic manner (Figure 2, inset). The ultrastructure of isolated stress fibers appeared to be comparable to that of stress fibers in cultured cells.

Composition of Isolated Stress Fibers

Isolated stress fibers that were still attached to coverslips were stained with fluorescein-labeled phalloidin (Figure 3a), and they were also recorded by video-enhanced phase-contrast microscopy (Figure 3b). Note that what remains of the cell after washes with extraction buffers I and II is basal stress fibers. Stress fibers purified by sucrose gradient centrifugation were stained with fluorescein-labeled phalloidin (Figure 3, c and e). By both phase-contrast (Figure 3d) and fluorescence microscopy (Figure 3e), the dimension of fractionated stress fibers was comparable to that of stress fibers in the cell. Attached stress fibers were double labeled with phalloidin (Figure 3f) and anti-vinculin (Figure 3g). Intense anti-vinculin staining was detected at the ends of stress fibers together with less-intense staining along their lengths in a dotted manner. Isolated stress fibers also showed the similar anti-vinculin staining pattern (Figure 3h). When paraformaldehyde-fixed cultured cells were stained with anti-myosin (Figure 4a) or anti-α-actinin (Figure 4b), banding patterns on stress fibers were visible. Isolated stress fibers stained with anti-myosin (Figure 4c) and anti-α-actinin (Figure 4d) also showed discontinuous dotty patterns along them. Anti-myosin light chain kinase (Figure 4e), anti-calmodulin (Figure 4f) and anti-vimentin (Figure 4g) also stained isolated stress fibers, often showing a dotty pattern. Although the data are not presented here, isolated stress fibers showed immunoreactivity with anti-filamin, anti-talin, anti-pp125^{FAK}, anti-integrin β_1 subunit, and anti-fibronectin receptor ($\alpha_5\beta_1$). Interestingly, paxillin appeared to have been extracted during the isolation procedure, because only a very weak anti-paxillin staining was associated with isolated stress fibers.

Fractionated stress fibers were analyzed by SDS gel electrophoresis. As shown in Figure 5a, compared with the whole-cell extract (Figure 5a, lane 1) and the TEA-treated extract (Figure 5a, lane 2), the isolated stress fiber fraction contained a limited number of polypeptides (Figure 5a, lane 3). We identified a total of 20 bands in the isolated stress fiber. To identify some of these components, we performed immunoblotting analyses using anti-α-smooth muscle actin, anti-α-actinin, anti-vinculin, anti-vimentin, anti-pan-myosin, and anti-fibronectin (Figure 5b). The results indicate that the 240-, 200-, 125-, 100-, 56-, and 45-kDa bands are fibronectin, myosin, vinculin, α-actinin, vimentin, and actin, respectively. Myosin light chain kinase and calmodulin bands could not be detected as silver-stained bands (Figure 5a). These proteins, however, were detected by immunoblotting (Figure 5, c and d, lane 1), the results consistent with the immunofluorescence staining data. The identity of other prominent bands, such as the 150- and 70-kDa bands, could not be determined.

We have earlier shown that fodrin, the nonerythrocyte type of spectrin, is in the cell cortex of cultured mammalian cells, but that the protein is excluded from the cell cortex where stress fibers are located (Katoh *et al*., 1996). Thus, the absence of fodrin in our isolated stress fiber preparation would be a good test for showing that the isolated are not contaminated with the general cell cortex. The same amounts (5 μg/lane) of fractionated stress fibers and a crude fibroblast extract were separately electrophoresed in the presence of SDS and immunoblotted using anti-α-spectrin (Figure 5e) or anti-α-fodrin. Little or no immunoreactivity was detected in the stress fiber fraction (Figure 5e, lane 1), whereas the cell extract exhibited a positive immunoreactivity for α-spectrin (Figure 5e, lane 2). These results strongly suggest that for all practical purposes, the isolated stress fiber fraction is free of the general cell cortex.

Figure 1 (facing page). Electron micrographs of negatively stained stress fibers isolated from bovine endothelial cells (a–c) or human foreskin fibroblasts (d). In a, one whole isolated stress fiber is

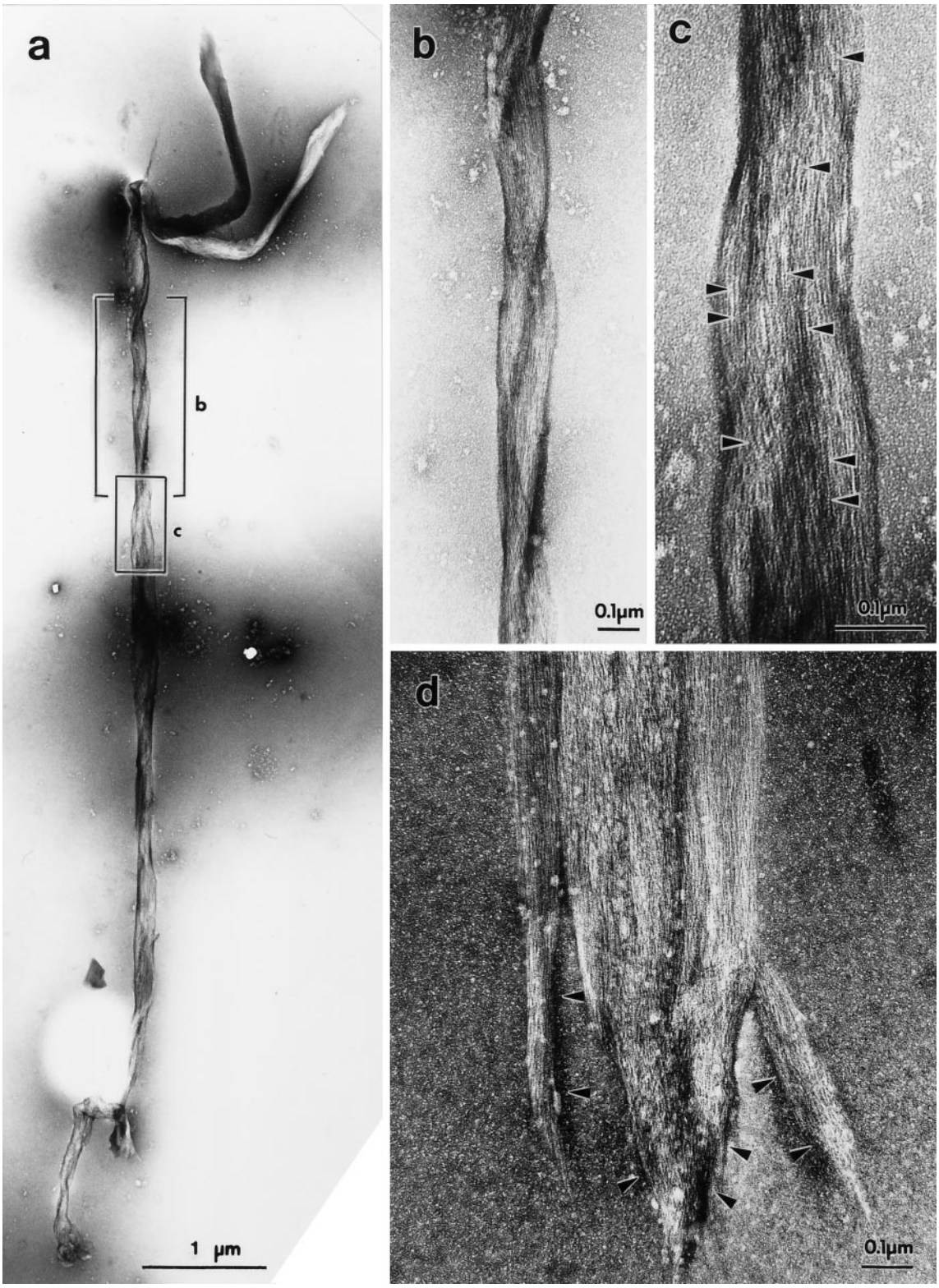

Figure 1 (cont). shown. Two boxed areas in a are enlarged and shown in b and c. Isolated stress fibers consisted of bundles of thin microfilaments. Globular actin monomers in individual filaments are clearly seen (c, arrowheads). Note that the stress fiber in a shows gentle twisting (better shown in b). The ends of isolated stress fibers showed distinct specialization, such as enlargement (a) and finger-like projections (d, arrowheads).

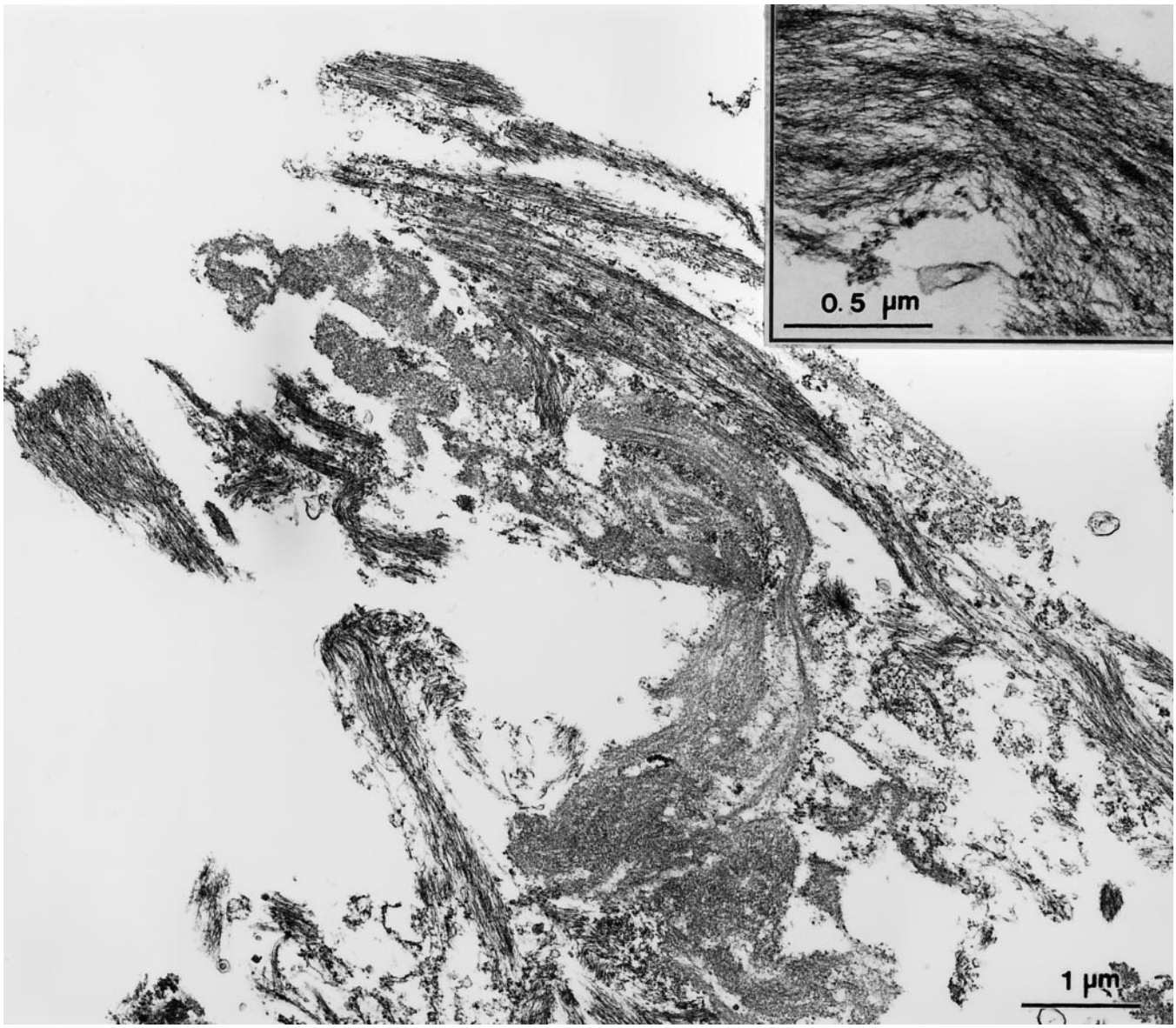

Figure 2. Conventional transmission electron micrographs of stress fibers isolated from human foreskin fibroblasts. A low-power view shows bundles of filaments cut in both longitudinal and cross-sectional directions. The morphology of isolated stress fibers is similar to that of in vivo stress fibers. In a high-power view, semiperiodic electron-dense regions within a microfilament bundle are visible (inset). This structure is one of the morphological characteristics of stress fibers.

Shortening of Isolated Stress Fibers

When isolated, free-floating stress fibers were treated with Mg-ATP, they shortened and formed small elliptical structures. To study the length change, we fixedand stained fractionated stress fibers with rhodamine-labeled phalloidin before or after Mg-ATP induced shortening. In Figure 6, inset, two typical isolated stress fibers are shown. The long stress fiber was present in a sample before the addition of Mg-ATP, whereas the short one is an example of stress fibers treated with Mg-ATP for 10 min. Because shortening of free-floating individual stress fibers was difficult to follow, we analyzed the distribution of stress fiber lengths with or without 10 min. Mg-ATP incu-

Figure 3 (facing page). F-actin and vinculin distribution in isolated stress fibers. Attached stress fibers stained with fluorescein-labeled phalloidin (a) and a video-enhanced phase-contrast image of the same sample (b) are shown. Fractionated stress fibers stained with fluorescein-labeled phalloidin (c and e) and a video-enhanced phase-contrast image of a small tangle of isolated stress fibers in the same fraction as in c (d) are shown. Double staining of attached

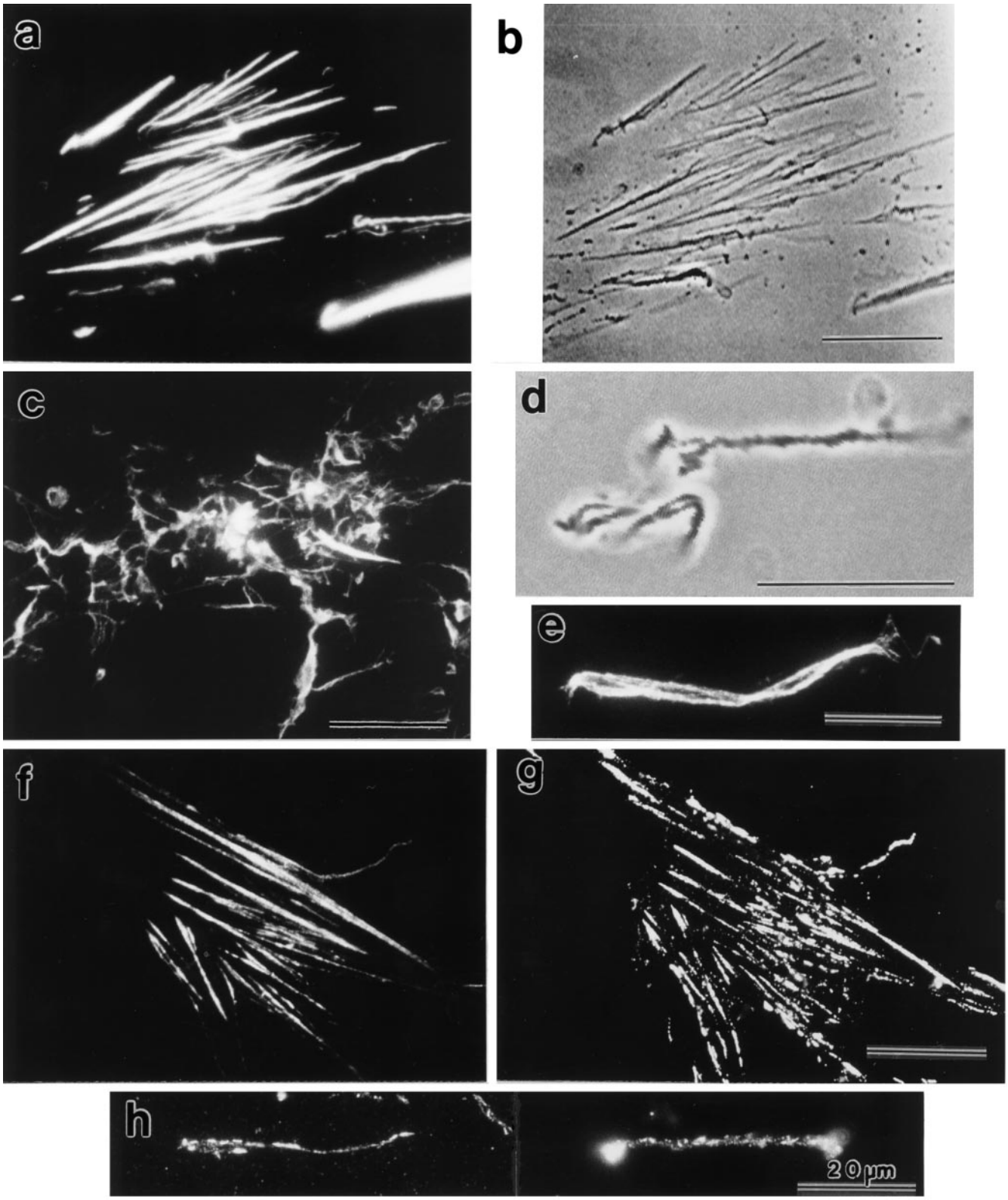

Figure 3 (cont). stress fibers with fluorescein-labeled phalloidin (f) and anti-vinculin (g) is shown. Fractionated stress fibers stained with anti-vinculin are shown (h). Note the dotty anti-vinculin staining pattern along the stress fibers (h).

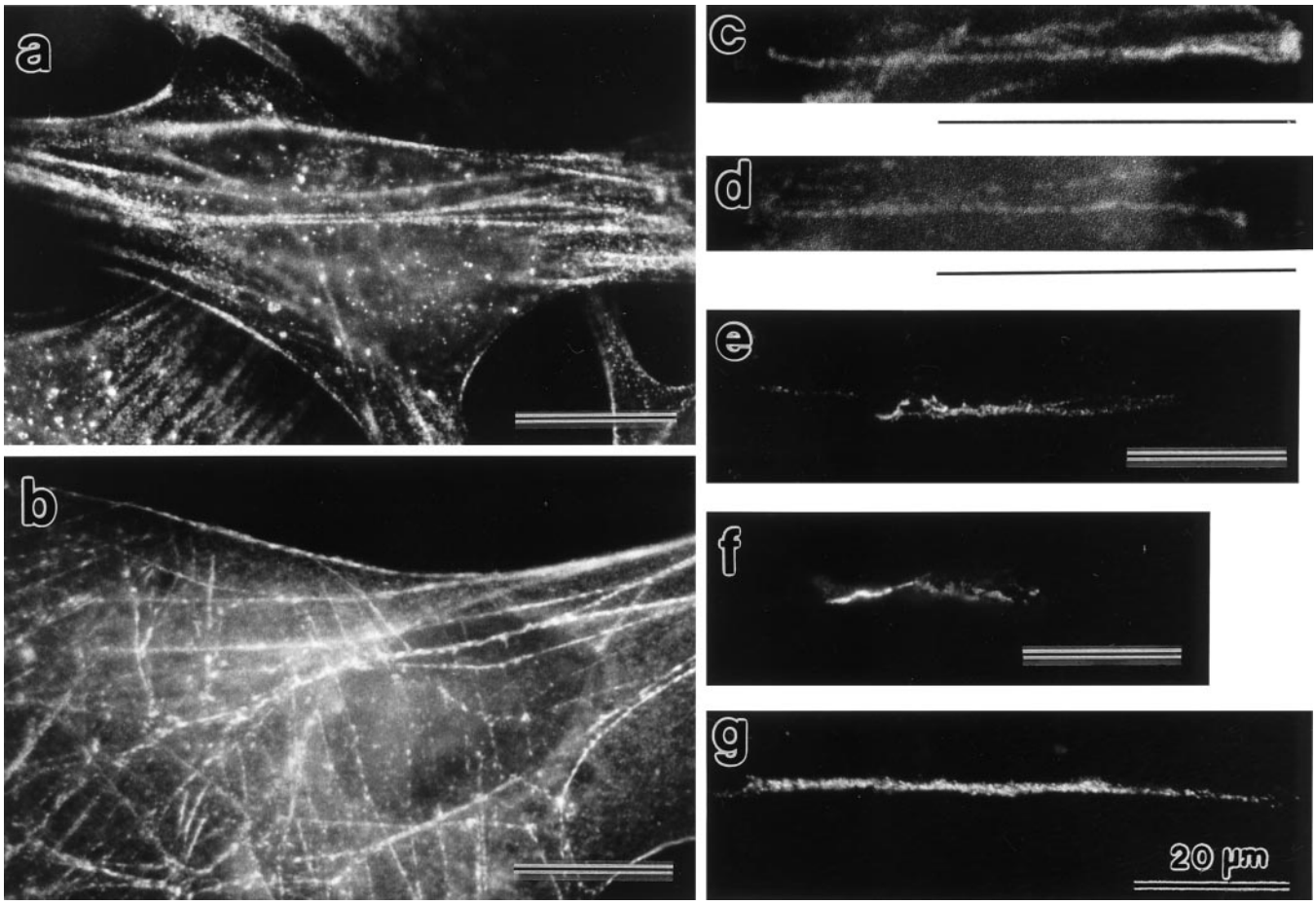

Figure 4. Myosin, α-actinin, myosin light chain kinase, calmodulin, and vimentin distribution in isolated stress fibers. Paraformaldehyde-fixed cells stained with anti-myosin (a) or anti-α-actinin (b) show a dotty pattern along the stress fiber. Fractionated stress fibers stained with anti-myosin (c) or anti-α-actinin (d) are shown. Note that isolated stress fibers also show dotty staining patterns. Anti-myosin light chain kinase (e), anti-calmodulin (f), and anti-vimentin (g) staining were also detected in isolated stress fibers with some dotty patterns.

bation. For each group, 500 stress fibers were measured. The length of shortened stress fibers was defined as the long axis of the elliptical fluorescent structure. The length of free-floating stress fibers before shortening was quite variable, its average being 91.7 ± 40.4 μm (Figure 6a, shaded bars). On the other hand, the mean length of shortened stress fibers was 21.5 ± 12.6 μm, and their distribution was quite narrow (Figure 6a, black bars). On average, therefore, an isolated stress fiber shortened to 23% of its original length.

We attempted to follow Mg-ATP-induced shortening of a single fractionated stress fiber. However, this was difficult to do as free-floating stress fibers moved about during their shortening. Thus, to study individual stress fiber shortening, we used attached stress fibers. Because such stress fiber preparations were not easily visible under the normal type of light microscopy, we used a video-enhanced phase-contrast microscopy to clearly observe them.

Attached stress fibers also shortened when they were exposed to Mg-ATP. They began to shorten within 3 s after the Mg-ATP buffer was perfused from one side of a coverslip, and shortening completed within 10–20 min. Examples of stress fiber shortening are shown in Figure 6, b and d. The final lengths of stress fibers were variable, but they shortened to 5–30% of the original length. The length change of the stress fiber shown in Figure 6b is plotted against time and shown in Figure 6c. In this case, the length reached was 19.7% of the original length after 5 min. Stress fiber shortening was biphasic. More than 50% shortening was achieved in ~30 s, and the rest of shortening took several minutes. The maximum speed of shortening in the example shown in Figure 7, a and b, was 2.4 μm/s. Other stress fibers also shortened at the similar maximum speed.

As seen in Figure 6, a and d, some phase-dark material was left behind on the coverslip after the attached stress fibers had shortened. This material

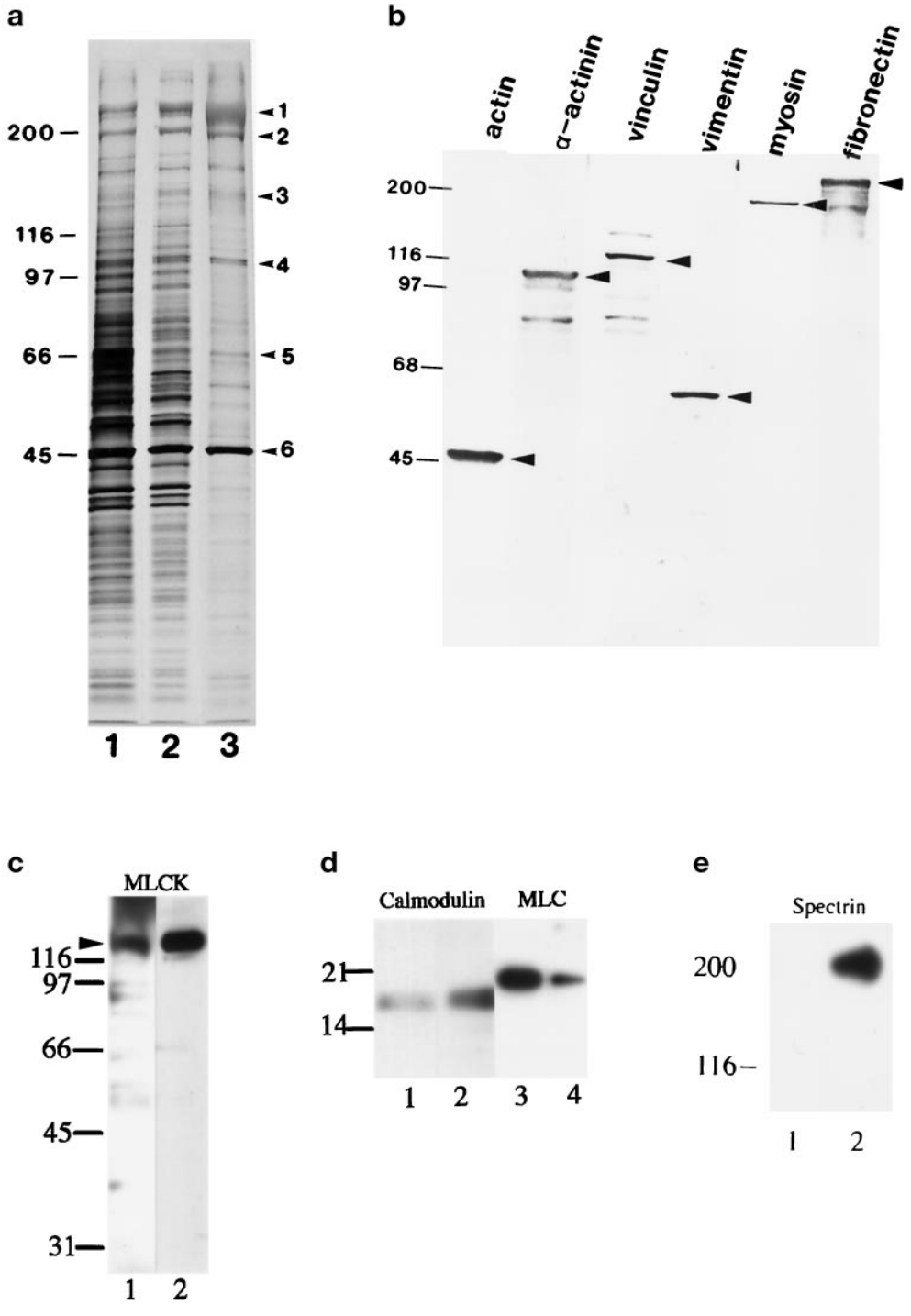

Figure 5. Gel electrophoresis and immunoblotting of isolated stress fibers. SDS-PAGE gels of a crude extract of fibroblasts (a, lane 1), a TEA-treated cell fraction (a, lane 2), and fractionated stress fibers (a, lane 3) are shown after silver staining. The identity of six major bands (1, fibronectin; 2, myosin; 3, vinculin; 4, α-actinin; 5, vimentin; and 6, actin) in the isolated stress fiber (a, lane 3, arrowheads) was determined by immunoblotting (b). Antibodies used in the immunoblotting analyses in b were anti-α-smooth muscle actin, anti-α-actinin, anti-vinculin, anti-vimentin, anti-myosin, and anti-fibronectin. The presence of myosin light chain kinase (c), calmodulin (d, lanes 1 and 2) and myosin regulatory light chain (d, lanes 3 and 4) was also detected by immunoblotting. Fractionated stress fibers (c, lane 1; d, lanes 1 and 3) and a crude extract of guinea pig aorta as a positive control (c, lane 2; d, lanes 2 and 4) were immunoblotted with anti-myosin light chain kinase (c), anti-calmodulin (d, lanes 1 and 2) and anti-myosin regulatory light chain (d, lanes 3 and 4). Fractionated stress fibers (e, lane 1) and a crude extract of fibroblasts (e, lane 2) were immunoblotted with anti-α-spectrin. Note that no immunoreactivity was detected in the stress fiber sample. Arrowheads in b and c indicate the position of the intact antigen bands.

could be a part of each stress fiber which had split longitudinally as the rest of it shortened. This could occur if the basal part of a stress fiber is tightly associated with the glass surface and/or some extracellular matrix. Another possibility is that this material is the extracellular matrix organized under the stress fiber. Immunoblotting (Figure 5b) data show that fibronectin is associated with isolated stress fibers. The presence of an organized extracellular matrix structure under the stress fiber may become apparent after stress fibers have shortened. The third possibility is that the material left behind consists of both split

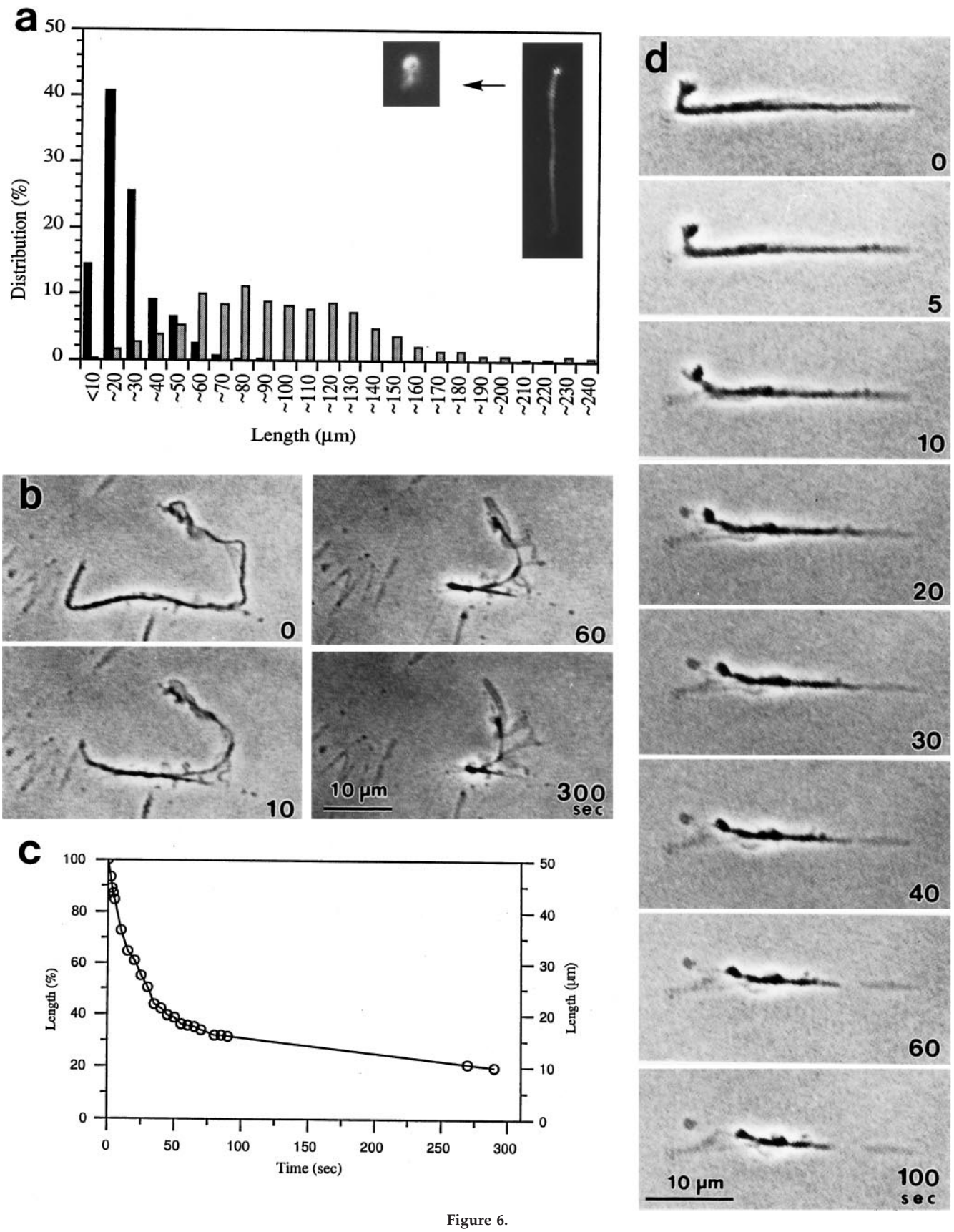
a
Distribution (%)
Length (μm)
<10
~20
~30
~40
~50
~60
~70
~80
~90
~100
~110
~120
~130
~140
~150
~160
~170
~180
~190
~200
~210
~220
~230
~240
b
0
60
10
10 μm
300 sec
c
Length (%)
Length (μm)
Time (sec)
d
0
5
10
20
30
40
60
10 μm
100 sec

Figure 6.

stress fibers and the extracellular matrix. When Mg-ATP-perfused samples were stained doubly with rhodamine-labeled phalloidin (Figure 7a) and anti-fibronectin (Figure 7b), the fibrous carpet-like material (Figure 7c) was intensely stained with anti-fibronectin. Phalloidin staining was observed near the center of this carpet, where shortened stress fibers were present. No phalloidin staining was detected in the outer areas of the carpet, suggesting that the entire stress fiber, not a part of it, shortened. These observations indicate that the material still adhering to the glass surface after stress fibers have shortened is not a part of stress fibers but is the extracellular matrix consisting of fibronectin.

Phosphorylation of the Myosin Regulatory Light Chain

Stress fiber shortening was dependent on the presence of Ca^{2+} because it was not observed in the contraction buffer containing 2 mM EGTA without $CaCl_2$. When stress fibers first treated with Mg-ATP were exposed to the relaxation solution, their length did not change during our observation time, which was 20 min. This result indicates that shortened stress fibers cannot lengthen or relax. To investigate nucleotide specificity for stress fiber shortening, ATP was replaced with various analogs. We found that 0.1 mM GTP, ADP, GDP, or AMP-PNP was ineffective in inducing stress fiber shortening. However, when stress fibers were incubated with 0.1 mM UTP, they shortened slowly and only slightly. When isolated stress fibers were incubated with 0.1, 0.05, 0.01, or 0.005 mM Mg-ATP, concentration-dependent shortening was observed (Figure 8a). Both the rate and the extent of shortening were affected by the low concentrations of ATP (0.01–0.05 mM). No shortening was induced by 0.005 mM ATP.

KT5926 is a myosin light chain kinase inhibitor, and stress fiber shortening was inhibited by this drug. When attached stress fibers were treated with 50, 100, 1000, or 5000 nM KT5926 for ≥30 min and then with 0.01 mM Mg-ATP, the rate (Figure 8b) and the extent (Figure 8c) of shortening were inhibited in a concentration-dependent manner. Stress fibers treated with Mg-ATP in the presence of 1 μM staurosporine, a protein kinase inhibitor, also failed to shorten. The state of phosphorylation of the myosin regulatory light chain in isolated stress fibers was investigated. Although the myosin regulatory light chain in isolated stress fibers was phosphorylatable (Figure 9, lane 2),

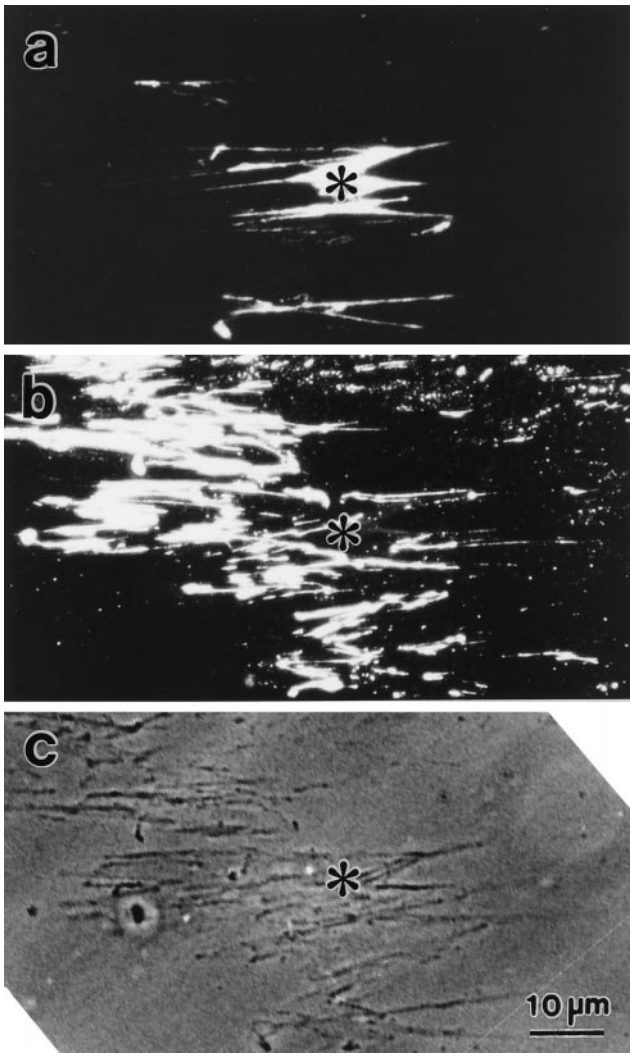

Figure 7. Identification of the material left behind shortening stress fibers. Attached stress fibers were treated with Mg-ATP, fixed, and stained doubly with rhodamine-labeled phalloidin (a) and anti-fibronectin (b). A video-enhanced phase-contrast image of the same field of view is shown in c. Phalloidin staining shows contracted stress fibers in the center of the micrograph (a), but the fibrous anti-fibronectin pattern occupies a wide portion of the field (b). Note that the anti-fibronectin staining structures are detectable in the phase-contrast micrograph (c). Asterisks indicate the same position in the three micrographs.

Figure 6. (facing page). Shortening of free-floating and attached stress fibers. Length distribution (percent) of free-floating isolated stress fibers before (shaded bars) and 10 min after (black bars) the addition of Mg-ATP were plotted (a). Length measurements were done using stress fibers fixed and stained with rhodamine-labeled phalloidin. The total number of isolated stress fibers counted for each type is 500. A typical example of free-floating isolated stress fiber either before or after shortening is shown in the inset (a). Isolated stress fibers still attached to glass surface were treated with Mg-ATP (b and d). The number in each frame indicates time in seconds after the addition of Mg-ATP solution. Note that the thickness of stress fibers decreases as they shorten. Note also some material left behind shortening stress fibers. The length change (expressed in percent of the initial length and also in actual length) of the stress fiber shown in b is plotted against time in c. The initial maximum speed of shortening was 2.4 μm/s, and the degree of shortening was 80% after 5 min.

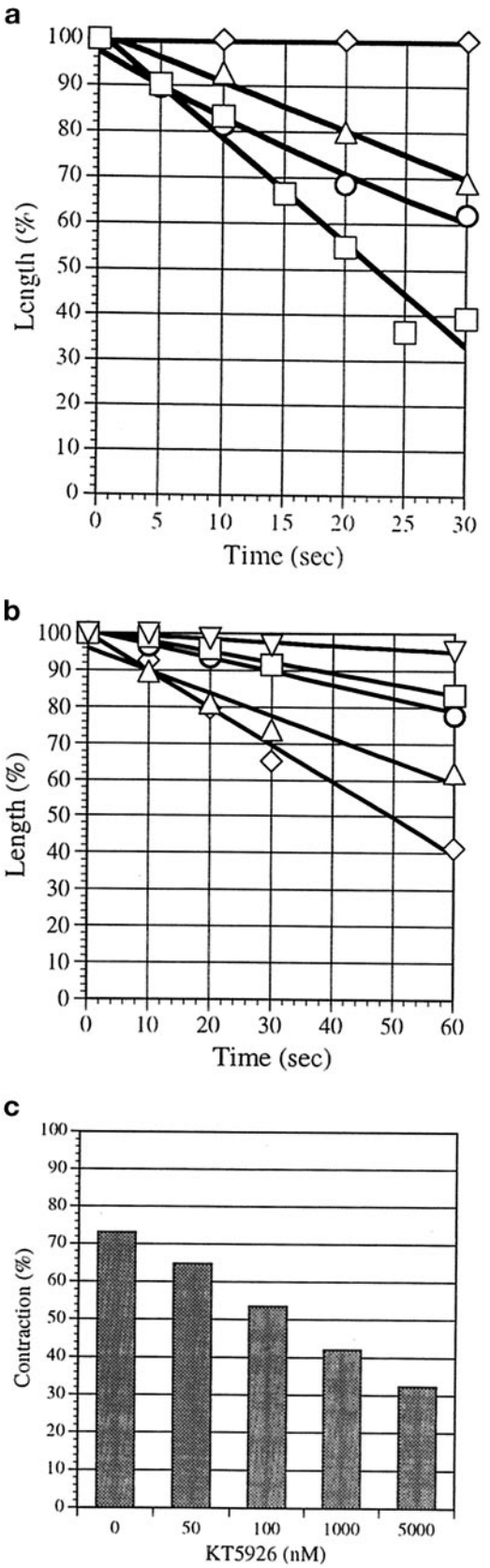

100 nM (Figure 9, lane 3) or 5000 nM (Figure 9, lane 4) KT5926 significantly decreased the extent of the light chain phosphorylation. These inhibitor experiments indicate that myosin regulatory light chain phosphorylation is involved in isolated stress fiber shortening.

No Actin Filament Dissociation during Stress Fiber Shortening

Because the degree of Mg-ATP-induced shortening of isolated stress fibers was extensive (Figure 6), actin filament dissolution was suspected. Thus, we examined whether monomeric actin was released into the contraction solution. A fractionated stress fiber preparation was divided into four equal aliquots, and stress fibers were collected by centrifugation at 100,000 $\times$ *g* for 1 h. Each pellet was resuspended into 100 μl of 0.1 mM ATP, ADP, AMP-PNP, or wash solution and incubated for 10 min at room temperature. Each sample was separated into a pellet and a supernatant by ultracentrifugation (100,000 $\times$ *g*) for 1 h. Pellets were resuspended into 100 μl of TBS. To all the pellets and supernatants, 100 μl of 2$\times$ SDS sample buffer were added. Exactly 10 μl of each gel sample were loaded onto a gel and electrophoresed. Gels were stained with SYPRO-orange, and the relative amounts of F-actin in the pellet and supernatant from each experiment are shown in Figure 10. Actin found in the supernatant after 10 min of shortening (Figure 10, ATP) was ~5.0%, but more importantly, the same amount of actin was also found in the supernatants of all the other cases. These results indicate that shortening of stress fibers occurs without F-actin dissolution.

Morphological Changes Associated with Stress Fiber Shortening

Observing stress fibers that were shortening, we noted that they became much thinner than they originally were (see Figure 6, b and d). Both replica electron microscopy and video-enhanced polarization micros-

Figure 8. The extent of stress fiber shortening depends on Mg-ATP concentration, and the effect of a myosin light chain kinase inhibitor, KT5926, inhibits stress fiber shortening. Isolated stress fibers still attached to glass surface were incubated with 0.1 mM (□), 0.05 mM (○), 0.01 mM (△), or 0.005 mM (◇) Mg-ATP solution, and their lengths were measured during shortening (a). These measurements were made from video images. Length is expressed in percent of the initial length. Mg-ATP at 0.1 mM induced >50% shortening within 30 s. Mg-ATP at 0.01 but not 0.005 mM was sufficient to induce shortening. Attached stress fibers were preincubated with no (◇), 50 nM (△), 100 nM (○), 1000 nM (□), or 5000 nM (▽) KT5926 for 30 min and then treated with 0.01 mM Mg-ATP. The length change measured from video recording is shown in b. The length is expressed as percent of the initial length. For each datum point, 20 stress fibers were measured. As the KT5926 concentration increased, stress fibers shortened more slowly. The extent of stress fiber shortening after 5 min of treatment with various concentrations of KT5926 is shown (c). Attached stress fibers were incubated with the indicated concentrations of KT5926 for 30 min and then with 0.01 mM Mg-ATP. After 5 min, the extent of shortening was measured. For each datum point, 20 stress fibers were measured. In this figure, the amount of shortening in percentage of the original length is shown.

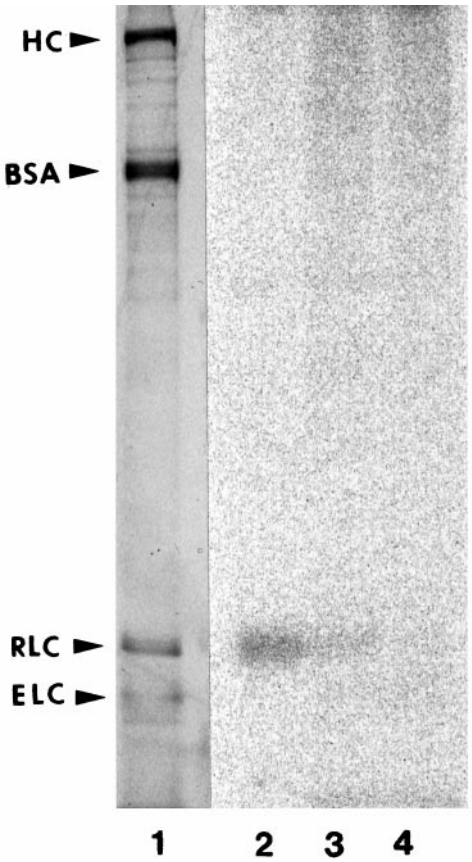

Figure 9. Phosphorylation of the myosin regulatory light chain in the isolated stress fiber. Fractionated stress fibers were preincubated with 0 (lane 2), 100 (lane 3), or 5000 nM (lane 4) KT5926 for 30 min on ice and then incubated with Mg-[γ-^{32}P]ATP. Purified chicken gizzard heavy meromyosin (HMM) mixed with BSA was used as a molecular marker (lane 1). Phosphorylation of the myosin regulatory light chain is inhibited by KT5926 in a concentration-dependent manner. HC, HMM heavy chain; RLC, myosin regulatory light chain; ELC, myosin essential light chain.

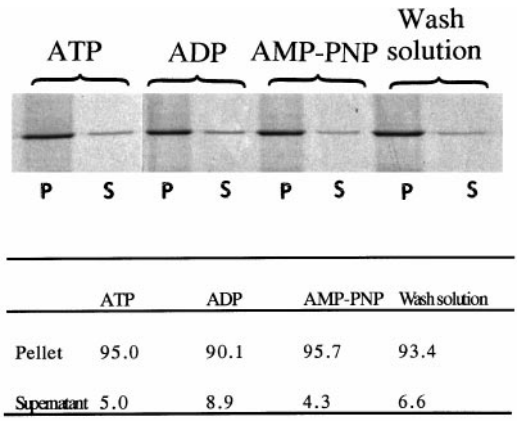

	ATP	ADP	AMP-PNP	Wash solution
Pellet	95.0	90.1	95.7	93.4
Supernatant	5.0	8.9	4.3	6.6

Figure 10. Absence of F-actin dissolution during shortening of isolated stress fibers. Fractionated stress fibers were treated with Mg-ATP, ADP, AMP-PNP, or wash solution. Centrifuged pellets (P) and supernatants (S) were electrophoresed and stained with SYPRO-orange. Actin bands are shown here. Relative amounts (in percent) of actin in the supernatants and the pellets were calculated from intensities of actin bands (table). Note that no dissolution of F-actin is caused by shortening.

copy were used to study structural changes of stress fibers before and after shortening. By replica electron microscopy, a stress fiber before shortening consisted of a loosely arranged bundle of microfilaments (Figure 11a). In this micrograph, individual microfilaments that are thickened by platinum and carbon coating are easily distinguishable. On the other hand, when stress fibers were perfused with Mg-ATP and then fixed, microfilaments in them were tightly compacted and were difficult to distinguish individually (Figure 11b). A low-power view of a stress fiber after shortening is shown in Figure 11c. This stress fiber (Figure 11c, asterisk) appears to have shortened from the left side and became a short, compact, oblong structure. It also appears that this stress fiber has flipped over from left to right, so that the right end used to be on the left. The position about which this flip might have occurred (Figure 11c, arrows) is presumably the strongest stress fiber–extracellular matrix attachment point. Such a flip would suggest tight coiling of the actin filament bundle during shortening of the stress fiber. Some filamentous structures (Figure 11c, arrowheads) remained on the glass surface are likely to be or consist of fibronectin (see Figure 7). In many cases, several stress fibers of the smaller caliber clearly showed evidence for tangling after Mg-ATP treatment (Figure 11d). Moreover, the surface of shortened stress fibers did not appear smooth, and at a high magnification, the surface was covered with many bleb-like structures (Figure 11e). These structures might be knots formed by tight winding of a microfilament bundle of the stress fiber. Thus, both tangling of several stress fibers and knot formation suggest vigorous winding or spinning of stress fibers during shortening.

Spinning Motion of Contracting Stress Fibers

To examine the mode of shortening of a single stress fiber, microbeads were attached to stress fibers, and their movement was recorded by video-enhanced phase-contrast microscopy and analyzed. When Mg-ATP solution was perfused, stress fibers shortened while carrying attached beads (Figure 12). All the beads attached to the same stress fiber eventually came to a spot, where the stress fiber presumably made the strongest attachment with the extracellular matrix. Where beads accumulated was not necessarily at one of the ends of a stress fiber. Often it occurred near the center of a stress fiber. These observations clearly indicate that stress fibers are shortening by contraction.

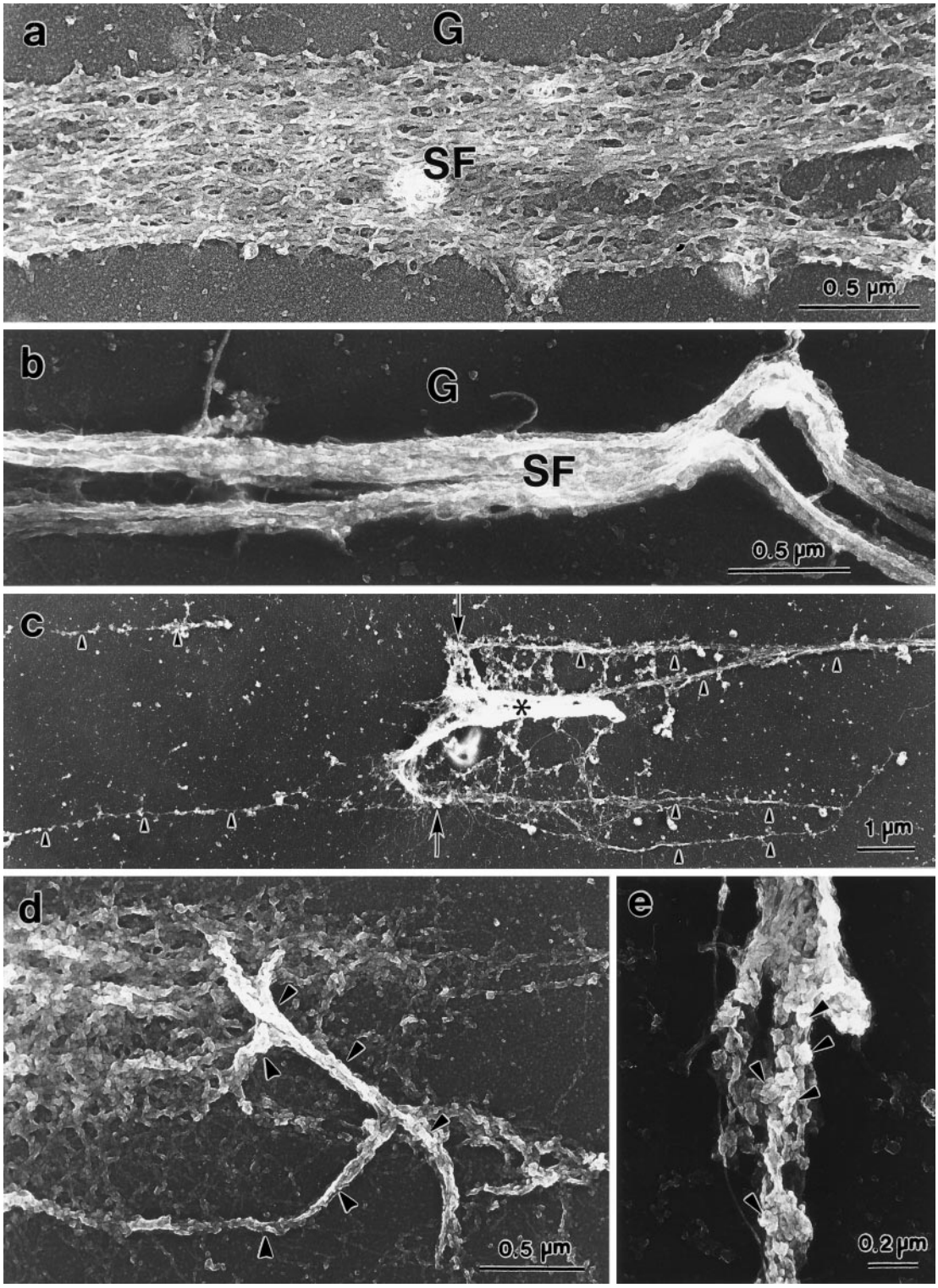

Figure 11. Replica electron microscopy of isolated stress fibers before and after Mg-ATP treatment. A loose bundle of microfilaments of an isolated stress fiber before Mg-ATP addition is shown (a). Individual microfilaments can be observed. After Mg-ATP addition, microfilaments in a bundle were no longer loose but were tightly packed (b). (c) Low-power view of an attached stress fiber at the end of shortening. The stress fiber (asterisk) is short and dense. It appears to have "contracted" from the left side of the micrograph and flipped over at the end about an imaginary line indicated by the two arrows. Note the extracellular matrix materials on the glass surface (c, arrowheads). Tangled stress fibers (d, arrowheads) and stress

During contraction of stress fibers, we often observed rotation of beads that were attached to them (Figure 12). Rotation was often jerky and easily went out of focus. Figure 12 shows two examples of bead rotation that occurred within the same plane of focus. These beads appear to be near the strongest attachment site of stress fibers, which helps them stay in focus. Because such a stress fiber portion can move (i.e., contract) only a short distance, the bead rotation seen is also modest. Nevertheless, in both cases, rotating motion of beads is clearly demonstrated (Lin *et al.*, 1984).

DISCUSSION

Isolation of Stress Fibers

Nonmuscle cells and tissues are known to form structures consisting of bundles of actin filaments, such as the contractile ring in dividing animal cells, the circumferential actin bundle in epithelial tissues, and the microvillus or the brush border. Mass isolation of these structures has been accomplished, enabling us to do biochemical and functional analyses of these contractile/cytoskeletal structures. The stress fiber is another structure made up of a bundle of actin filaments. However, this actin bundle-containing structure has not been isolated in mass, and our knowledge on this intriguing cytoskeletal system has been largely limited to its morphology. The formation and the maintenance of stress fibers in cells depend on the presence of tension (Burridge and Chrzanowska-Wodnicka, 1996). Dynamic assembly and disassembly of stress fibers by tension have been reported (Mochitate *et al.*, 1991; Halliday and Tomasek, 1995). These observations seem to indicate that the stress fiber is a rather labile structure that requires tension to keep its integrity and that it might not be isolatable once tension is released. However, in this report, we show that stress fibers can be isolated without making any special attempts to stabilize them. This indicates that the stress fiber is reasonably stable. Furthermore, it can be cleanly separated from the rest of the cell, indicating that it is an independent structure (i.e. an organelle), not a specialized region of the cell cortex, as we have earlier suggested (Fujiwara *et al.*, 1985).

There were two important steps in the isolation procedure that contributed to the successful purification of stress fibers. One was the use of TEA, which caused dissolution and/or disruption of cells except for the stress fiber and the focal adhesion together with fibronectin fibers. The other was freeing individual stress fibers by shearing the sheet-like material collected from culture dishes.

Fractionated stress fibers had the same basic morphology as those in cultured cells when examined by conventional electron microscopy. Analyses using specific antibodies indicated that isolated stress fibers, like those in the cell, contained major contractile proteins as well as proteins present at the stress fiber–plasma membrane association site. Although paxillin was easily extracted by the isolation procedure, our investigation revealed that no other major polypeptides known to be associated with stress fibers and focal contacts were absent in the isolated stress fiber. All these data suggest that the present protocol is not only the first mass isolation method for stress fibers but also useful for systematic analyses of the macromolecular organization of the stress fiber and its association sites with the plasma membrane.

By SDS-PAGE and silver staining, ~20 bands were detected in the purified stress fiber fraction. Immunoblotting experiments enabled us to identify six of them as fibronectin, myosin, vinculin, α-actinin, vimentin, and actin, but other components remain unknown. It is possible that novel proteins are enriched in this fraction. Using anti-tropomyosin and anti-α-actinin, Lin *et al.* (1984) purified microfilament-containing structure from homogenates of cultured cells. It is suspected that many of these structures are fragmented stress fibers. When we compare the SDS-PAGE patterns of the antibody-purified microfilaments (*Lin et al.*, 1984, their Figure 2, lane 5) and of our isolated stress fibers (Figure 5a, lane 3), they are indeed very similar. SDS-PAGE as well as immunofluorescence analyses revealed the presence of vimentin in the isolated stress fiber. The total amount of vimentin is rather substantial, but we were unable to identify 10-nm filaments in stress fibers by electron microscopy. Interestingly, Lin *et al.* (1984) also reported the presence of vimentin in their antibody-purified filaments. Immunofluorescence data suggest that this protein is distributed more or less uniformly along the stress fiber. Because anti-vimentin staining of cultured cells does not usually reveal the stress fiber pattern inside cells, the mode of vimentin organization in isolated stress fibers remains to be investigated. Because certain integrin subunits can bind to intermediate filaments (Sonnenberg *et al.*, 1991; Lee *et al.*, 1992), some vimentin intermediate filaments may be bound to integrins.

Stress fibers are also present in the apical portion of cultured cells (Buckley and Porter, 1967; Fujiwara and Pollard, 1976; Osborn *et al.*, 1978; Katoh *et al.*, 1995, 1996) and of cells in situ (White and Fujiwara, 1986; Kano *et al.*, 1996). These apical stress fibers are not included in our purified stress fiber fraction, because the TEA treatment and detergent extraction procedure effectively removes the entire dorsal part of the cell.

Figure 11 (cont). fibers exhibiting small, knot-like structures on the surface (e, arrowheads) are illustrated. G, glass surface; SF, stress fiber.

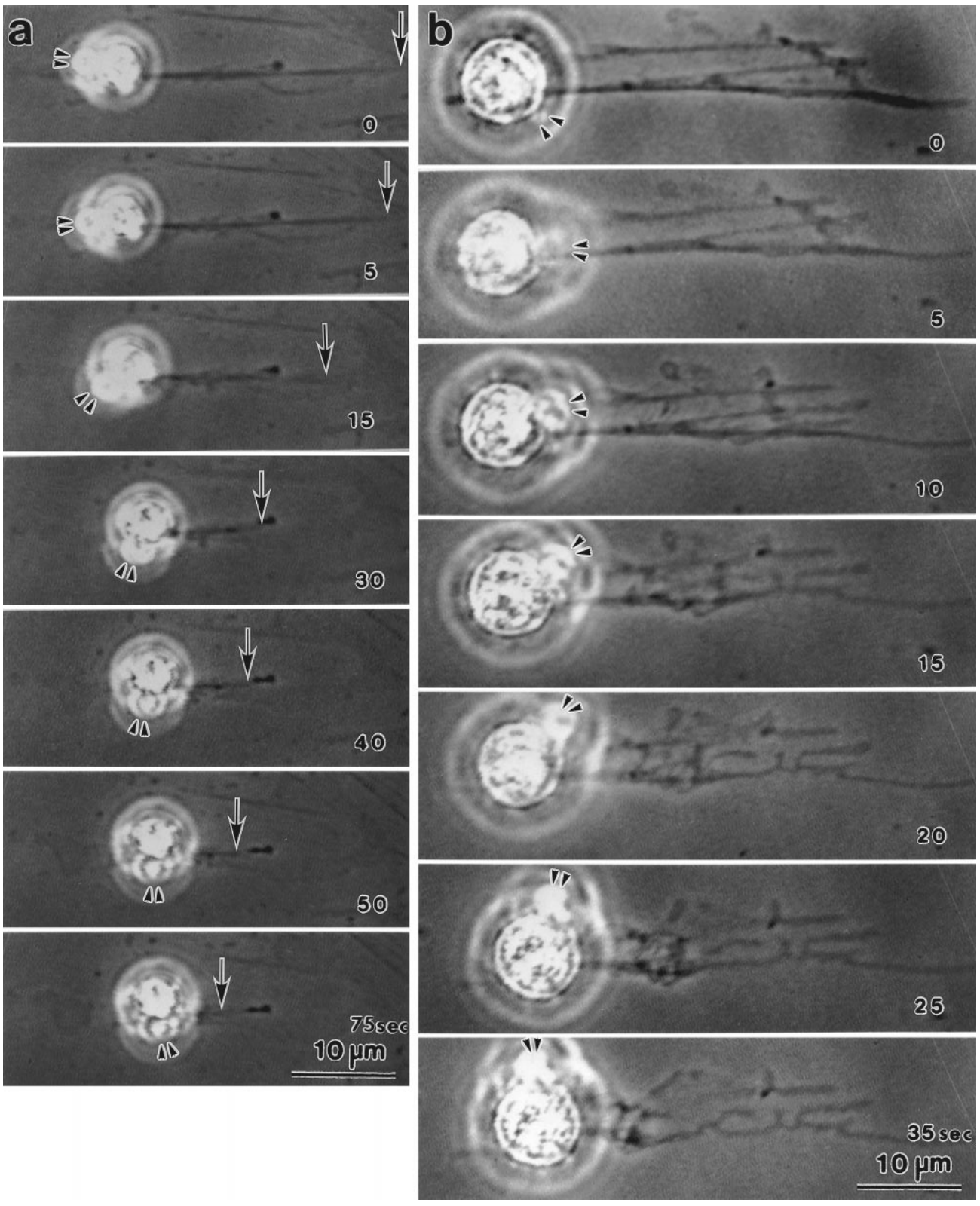

Figure 12. Rotation of microbeads during contraction of stress fibers. Microbeads were attached to isolated stress fibers to analyze the motion of shortening stress fibers. These video-enhanced phase-contrast images are from time-lapse recording using a disk recorder. The

This dorsal portion of the cell may be used to isolate apical stress fibers as well as apical plaques (Katoh *et al.*, 1995, 1996). Such an attempt has now been undertaken.

Contraction of Stress Fibers

Earlier experiments by Hoffmann-Berling (1954), Isenberg *et al.* (1976), and Kreis and Birchmeier (1980) have provided circumstantial evidence for stress fiber contractility, but there has been no direct evidence showing that stress fibers themselves can shorten by contraction. In this study, we have shown that the stress fiber is a truly contractile structure. First of all, we have found that isolated stress fiber shortening is dependent on ATP and Ca^{2+} and that it is inhibited by protein kinase inhibitors, one of which is specific for myosin light chain kinase (KT5926). During isolation procedures, stress fibers were in low-Ca^{2+}-concentration buffers and solution for typically $\geq$1 h. Under these circumstances, the regulatory light chain of myosin would be dephosphorylated. When Ca^{2+} and ATP are added, the light chain is likely to be phosphorylated by the action of calmodulin and myosin light chain kinase, both of which are associated with isolated stress fibers. Indeed, we have shown phosphorylation of the myosin regulatory light chain when stress fibers were treated with Ca^{2+} and Mg-ATP, and this phosphorylation was inhibited by KT5926. No massive F-actin dissolution during shortening of stress fiber was detected, indicating that the rapid stress fiber shortening is not due to actin filament depolymerization. These results indicate that stress fiber shortening is due to actomyosin contraction. Furthermore, several morphological changes, all of which indicate contraction of stress fibers, have been noted during stress fiber shortening. Before shortening, actin filaments in stress fibers were loosely packed. When Mg-ATP was added, actin filament packing first became tighter, making the diameter of each stress fiber smaller. During contraction, stress fibers rotated, as ascertained by bead rotation, and at the end, formed short, dense, rod-like structures. Knot formation observed with slender stress fibers also indicates that stress fibers spin during contraction. This is analogous to knot formation that occurs when a rubber band is tightly wound. Tangled stress fibers observed after contraction also indicate the presence of spinning movement among branching stress fibers.

Contractility of isolated cells and actomyosin-containing structures of nonmuscle cells has been reported and is summarized in Table 1. Except for smooth muscle cells and snapping tails of cultured cells, the speed of contraction is slow in general. Furthermore, many systems show a rather limited extent of shortening; often showing only 20–30% shortening. This is particularly true for the cell cortex models containing stress fibers. Our isolated stress fibers contracted to 23% of the original length. This extent of shortening is rather substantial, and we suggest that spiral contraction makes it possible for isolated stress fibers to shorten so extensively. The maximum speed of contraction was several micrometers per second. This rate of contraction is on the order similar to that of isolated smooth muscle cells, indicating that the stress fiber is a very efficient contractile apparatus. Our study reveals that the stress fiber is the fastest actomyosin-based contractile apparatus found in animal nonmuscle cells. Activity motile cultured cells, such as fibroblasts, often exhibit retraction of their so-called tails. This recoiling is one of the fastest contractile motions seen in nonmuscle cells. The maximum speed of tail retraction of cultured cells was reported to be several micrometers per second (Chen, 1981). As the author has pointed out, it is likely that the force for tail retraction is generated by stress fibers in the tail.

Biological Implications of Stress Fiber Contraction

Whether stress fibers in the cell also rotate as they contract is an interesting question. If tail recoiling is indeed caused by stress fiber contraction, this is a good system in which to investigate this point. A detailed study done by Chen (1981) did not describe tail spinning. Interestingly, however, he described that strongly birefringent tail lost its optical anisotropy after recoil. This may suggest that stress fibers in the tail form a knotted spiral at the end of tail retraction and that this is the reason why birefringence is lost. In this tail-recoiling system, retraction was induced by mechanically breaking the cell–substrate attachment at the tip of the tail. This may cause stress fibers to disengage themselves from the cell membrane and to contract in a spiral manner without transmitting the spiral motion to the entire tail.

As various investigators have predicted (see review by Burridge, 1981), stress fibers are truly contractile and, therefore, can indeed produce isomeric tension in the cell. This is possible only because both ends of stress fibers are anchored to the stiff substrate (glass or plastic surface in vitro and the basement membrane in vivo) via the focal adhesion. Thanks to this isometric contraction, stress fibers are able to function as a cytoskeletal system. The distance between two focal adhesions, each located at each end of a stress fiber, does

Figure 12 (facing page). number at the right bottom corner in each plate is time in seconds after Mg-ATP addition. Microbeads attached to the vicinity of one end of isolated stress fibers were selected for observation. Two examples are shown (a and b). The double arrowheads (a and b) indicate the same position on the bead clusters. The number in each panel indicates time in seconds after Mg-ATP addition.

Table 1. Actomyosin-based contractility of smooth muscle and nonmuscle cells

Contractile cells and apparatuses	Extent of contraction	Speed	References
Isolated stress fiber	100 → 23% (average)	Max: 2.4 μm/s (biphasic)	Present study
Cell model	100 → 60% (microlaser dissection)		Isenberg *et al*., 1976
	100 → 80% (glycerol extracted)		Kreis and Birchmeier, 1980
	100 → 80 ~ 75% (digitonin extracted)		
Circumferencial microfilament bundle	100 → 40%	8 ~ 10 μm/min at first 2 min	Owaribe and Masuda, 1982
Contractile ring		Max: 10 μ/min Average: 3.4 μm/min	Mabuchi *et al*., 1988
	12 → 3 ~ 4 μm (diameter change)		Cande, 1980
Brush border	25 × 10 μm (ellipse) → 10 ~ 15 μm (round) (diameter change)		Rodewald *et al*., 1976
Kidney proximal tubule	100 → 80% (Triton X-100 extracted)		Murakami and Ishikawa, 1991
Tail recoiling		Max: 3.5 μm/s[a] Average: 1.5 μm/s[a]	Chen, 1981
Smooth muscle cell	100 → 38%		Fay *et al*., 1982
		Average: 10 μm/s	Small, 1977

[a] Calculated from published data.

not change for cells in culture. However, for cells in vivo, this distance is not kept constant as the body moves. A structure that can operate isometrically is indeed an ideal skeletal system for cells in the body.

Hynes and Destree (1978) showed that patterns of the stress fiber distribution in a cultured cell and the fibronectin fibril organization under the same cell were often superimposable. However, because there were many cases in which this superimposability was apparently absent, this observation was often forgotten. Our study shows that the morphological association between the stress fiber and fibronectin is tight. Isolated stress fiber on the glass surface always had organized fibronectin underneath. We suggest that the stress fiber–fibronectin association is fundamental, not coincidental. Indeed, when we observe stress fibers in endothelial cells in situ, there is always linearly organized fibronectin under the cells, and the two patterns are superimposable (Jinguji and Fujiwara, 1994; Kano *et al*., 1996). We suggest that the rich deposition of fibronectin under cultured cells makes it difficult to clearly detect the stress fiber–fibronectin association in in vitro systems.

The basic macromolecular assembly of the stress fiber appears to be similar to that of the striated muscle sarcomere (Sanger, 1980; Langanger *et al*., 1986). Specialized features that characterize various differentiated cells can be traced back to the general structures and functions of undifferentiated cells, albeit they are expressed in far less organized and efficient manners in the latter cells. We suggest that the molecular organization of the most efficient contractile apparatus in undifferentiated and nonmuscle cells (i.e. the stress fiber) is adopted by the cell specialized for contraction. Thus, the basic macromolecular architecture of the sarcomere is found in the stress fiber. This idea has been proposed by many investigators in the past, but without clear demonstration of stress fiber contractility, it has not become a serious hypothesis in cell biology. Our study provides functional and strong support for the idea that the stress fiber is the prototype of the muscle fibril.

The ends of a stress fiber are anchored to focal adhesions. In the case of striated muscle cells, their myofibrils are anchored to the tendon for the skeletal muscle and to the intercalated disk for the cardiac muscle. Interestingly, many of the proteins found at the focal adhesion of cultured cells are also present at the muscle–tendon junction (Shear and Bloch, 1985) and the intercalated disk (Geiger *et al*., 1980). It is likely that each of these contractile apparatus–plasma membrane attachment site contains both the basic common supramolecular assembly needed to anchor actin filaments to the extracellular matrix through the plasma membrane and the molecules needed specifically for the functioning of each type of attachment sites. Because it is easiest to molecularly dissect the components of the focal contact site, this site is the best studied one. Our present study provides further means for investigating this important region of the cell.

ACKNOWLEDGMENTS

This work was supported in part by Grants in Aid for Scientific Research from the Ministry of Education, Science and Culture, Japan, grants from the Ministry of Health and Welfare of Japan, and Special Coordination Funds for Promoting Science and Technology (COE) from the Science and Technology Agency of Japan.

REFERENCES

Avnur, Z., and Geiger, B. (1981). Substrate attached membranes of cultured cells. Isolation and characterization of ventral membranes and the associated cytoskeleton. J. Mol. Biol. *153,* 361–379.

Avnur, Z., Small, V., and Geiger, B. (1983). Actin-independent association of vinculin with the cytoplasmic aspect of the plasma membrane in cell-contact areas. J. Cell Biol. *96,* 1622–1630.

Badley, R.A., Lloyd, C.W., Woods, A., Carruthers, L., and Allcock, C. (1978). Mechanisms of cellular adhesion. Exp. Cell Res. *117,* 231–244.

Ball, E.H., Freitag, C., and Gurofsky, S. (1986). Vinculin interaction with permeabilized cells: disruption and reconstruction of a binding site. J. Cell Biol. *103,* 641–648.

Brands, R., and Feltkamp, C.A. (1988). Wet cleaving of cell: a method to introduce macromolecules into the cytoplasm. Exp. Cell Res. *176,* 309–318.

Buckley, I.K., and Porter, K.R. (1967). Cytoplasmic fibrils in living cultured cells. Protoplasma *64,* 349–380.

Burridge, K. (1981). Are stress fibers contractile? Nature *294,* 691–692.

Burridge, K., and Chrzanowska-Wodnicka, M. (1996). Focal adhesions, contractility, and signaling. Annu. Rev. Cell Dev. Biol. *12,* 463–519.

Burridge, K., Fath, K., Kelly, K., Nuckolls, G., and Turner, C. (1988). Focal adhesions: transmembrane junction between the extracellular matrix and the cytoskeleton. Annu. Rev. Cell Biol. *4,* 487–525.

Byers, H.R., White, G.E., and Fujiwara, K. (1984). Organization and function of stress fibers in cells in vitro and in situ. Cell Muscle Motil. *5,* 83–137.

Cande, W.Z. (1980). A permeabilized cell model for studying cytokinesis using mammalian tissue culture cells. J. Cell Biol. *87,* 326–335.

Cathcart, M.K., and Culp, L.A. (1979). Initial studies of the molecular organization of the cell-substrate adhesion site. Biochim. Biophys. Acta *556,* 331–343.

Chen, W. (1981). Mechanism of retraction of the trailing edge during fibroblast movement. J. Cell Biol. *90,* 187–200.

Fay, F.S., Fogarty, K., Fujiwara, K., and Tuft, R. (1982). Contractile mechanism of single isolated smooth muscle cells. In: Basic Biology of Muscles: A Comparative Approach, ed. B.M. Dewey, New York: Raven Press, 143–157.

Fujiwara, K., and Pollard, T.D. (1976). Fluorescent antibody localization of myosin in the cytoplasm, cleavage furrow, and mitotic spindle of human cells. J. Cell Biol. *71,* 848–875.

Fujiwara, K., Porter, M.E., and Pollard, T.D. (1978). Alpha-actinin localization in the cleavage furrow during cytokinesis. J. Cell Biol. *79,* 268–275.

Fujiwara, K., White, G.E., and White, L.D. (1985). Role of in situ stress fibers in cellular adhesion. In: Cell Motility: Mechanism and Regulation, ed. H. Ishikawa, S. Hatano, and H. Sato, Tokyo: University of Tokyo Press, 477–492.

Geiger, B., Tokuyasu, K.T., Dutton, A.H., and Singer, S.J. (1980). Vinculin, an intracellular protein localized at specialized sites where microfilament bundles terminate at cell membranes. Proc. Natl. Acad. Sci. USA *77,* 4127–4131.

Halliday, N.L., and Tomasek, J.J. (1995). Mechanical properties of the extracellular matrix influence fibronectin fibril assembly in vitro. Exp. Cell Res. *217,* 109–117.

Harris, A.K., Stopak, D., and Wild, P. (1981). Fibroblast traction as a mechanism for collagen morphogenesis. Nature *290,* 249–251.

Hoffmann-Berling, H. (1954). Adenosintriphosphat als Betriebsstoff von Zellbewegungen. Biochim. Biophys. Acta *14,* 182–194.

Hynes, R.O., and Destree, A.T. (1978). Relationships between fibronectin (LETS protein) and actin. Cell *15,* 875–886.

Isenberg, G., Rathke, P.C., Hülsmann, N., Franke, W.W., and Wohlfarth-Bottermann, K.E. (1976). Cytoplasmic actomyosin fibrils in tissue culture cells. Direct proof of contractility by visualization of ATP-induced contraction in fibrils isolated by laser microbeam dissection. Cell Tissue Res. *166,* 427–443.

Jinguji, Y., and Fujiwara, K. (1994). Stress fiber dependent axial organization of fibronectin fibrils in the basal lamina of the chick aorta and mesenteric artery. Endothelium *2,* 35–47.

Kano, Y., Katoh, K., Masuda, M., and Fujiwara, K. (1996). Macromolecular composition of stress fiber-plasma membrane attachment sites in endothelial cells in situ. Circ. Res. *79,* 1000–1006.

Katoh, K., Kano, Y., Masuda, M., and Fujiwara, K. (1996). Mutually exclusive distribution of the focal adhesion associated proteins and the erythrocyte membrane skeleton proteins in the human fibroblast plasma membrane undercoat. Cell Struct. Funct. *21,* 27–39.

Katoh, K., Masuda, M., Kano, Y., Jinguji, Y., and Fujiwara, K. (1995). Focal adhesion proteins associated with apical stress fibers of human fibroblasts. Cell Motil. Cytoskeleton *31,* 177–195.

Kreis, T.I., and Birchmeier, W. (1980). Stress fiber sarcomeres of fibroblasts are contractile. Cell *22,* 555–561.

Laemmli, U.K. (1970). Cleavage of structural proteins during the assembly of the head of bacteriophage T4. Nature. *227,* 680–685.

Langanger, G., Moreremans, M., Daneels, G., Sobieszec, A., De Brabander, M., and De Mey, J. (1986). The molecular organization of myosin in stress fibers of cultured cells. J. Cell Biol. *102,* 200–209.

Lee, E.C., Lotz, M.M., Steele, G.D., Jr., and Mercurio, A.M. (1992). The integrin $\alpha 6\beta 4$ is a laminin receptor. J. Cell Biol. *117,* 671–678.

Lin, J.J., Mastumura, F., and Yamashiro-Matsumura, S. (1984). Tropomyosin-enriched and alpha-actinin enriched microfilaments isolated from chicken embryo fibroblasts by monoclonal antibodies. J. Cell Biol. *98,* 116–127.

Mabuchi, I., Tsukita, S., Tsukita, S., and Sawai, T. (1988). Cleavage furrow isolated from newt eggs: contraction, organization of the actin filaments, and protein components of the furrow. Proc. Natl. Acad. Sci. USA *85,* 5996–5970.

Mochitate, K., Pawelek, P., and Grinnell, F. (1991). Stress fiber relaxation of contracted collagen gels: disruption of actin filament bundles, release of cell surface fibronectin, and down-regulation of DNA and protein synthesis. Exp. Cell Res. *193,* 198–207.

Mooseker, M.S., and Tilney, L.G. (1975). Organization of an actin filament-membrane complex: filament polarity and membrane attachment in the microvilli of intestinal epithelial cells. J. Cell Biol. *67,* 725–743.

Murakami, T., and Ishikawa, H. (1991). Stress fibers in situ in proximal tubules of the rat kidney. Cell Struct. Funct. *16,* 231–240.

Nakanishi, S., Yamada, K., Iwahashi, K., Kuroda, K., and Kase, H. (1990). KT5926, a potent and selective inhibitor of myosin light chain kinase. Mol. Pharmacol. *37,* 482–488.

Neyfakh, A.A., and Svitkina, T.M. (1983). Isolation of focal contact membrane using saponin. Exp. Cell Res. *149,* 582–586.

Nicol, A., and Nermut, M.V. (1987). A new type of substratum adhesion structure in NRK cells revealed by correlated interference reflection and electron microscopy. Eur. J. Cell Biol. *43,* 348–357.

Osborn, M., Born, T., Koitsch, H., and Weber, K. (1978). Stereo immunofluorescence microscopy: I. Three-dimensional arrangement of microfilaments, microtubules and tonofilaments. Cell *14,* 477–488.

Owaribe, K., and Masuda, H. (1982). Isolation and characterization of circumferential microfilament bundles from retinal pigmented epithelial cells. J. Cell Biol. *95,* 310–315.

Rodewald, R., Newman, S.B., and Karnovsky, M.J. (1976). Contraction of isolated brush borders from the intestinal epithelium. J. Cell Biol. *70,* 541–554.

Sanger, J.M. (1980). Banding and polarity of actin filaments in interphase and cleaving cells. J. Cell Biol. *86,* 568–575.

Shear, C.R., and Bloch, R.J. (1985). Vinculin in subsarcolemmal densities in chick skeletal muscle: localization and relationship to intracellular and extracellular structures. J. Cell Biol. *101,* 240–256.

Small, J.V. (1977). Studies on isolated smooth muscle cells: the contractile apparatus. J. Cell Sci. *24,* 327–349.

Sonnenberg, A. *et al*. (1991). Integrin $\alpha 6/\beta 4$ complex is localized in hemidesmosomes, suggesting a major role in epidermal cell-basement membrane adhesion. J. Cell Biol. *113,* 907–917.

Sunada, H., Masuda, M., and Fujiwara, K. (1993). Preservation of differentiated phenotypes in cultured aortic endothelial cells by malotilate and phosphoascorbic acid. Eur. J. Cell Biol. *60,* 48–56.

White, G.E., and Fujiwara, K. (1986). Expression and intracellular distribution of stress fibers in aortic endothelium. J. Cell Biol. *103,* 63–70.

Yonemura, S., Mabuchi, I., and Tsukita, S. (1991). Mass isolation of cleavage furrows from dividing sea urchin eggs. J. Cell Sci. *100,* 73–84.